Mg-rich hollow sanidine in partially melted granite xenoliths in a mica peridotite at Rose dome, Woodson County, Kansas

MICHAEL P. SMITH[1] AND PAUL C. FRANKS

Department of Geosciences
University of Tulsa, Tulsa, Oklahoma 74104

Abstract

Hollow sanidine as much as 100 μm long enclosed in micropoikilitic quartz in Precambrian Rose dome granite, Woodson County, Kansas, probably grew from a supersaturated melt. The melt formed by the addition of heat and water to granite xenoliths from a Late Cretaceous mica-peridotite host. The granitic melt probably became supersaturated in sanidine due to a substantial loss of water from both the peridotite and granite melts upon emplacement. Universal-stage $2V_x$ measurements in the range 37–44° are consistent with a high-sanidine structure. Microprobe analyses show that the sanidine contains relatively high concentrations of Fe, Mg, and Si, and low Al. In contrast, relict K-feldspar has a more normal composition: MgO below detection limits and 0.04 wt.% FeO. The hollow sanidines, which contain more than three silica cations per eight oxygens, are, to the best of our knowledge, the most siliceous alkali feldspars ever analyzed.

Hollow calcic plagioclase has been reported from lunar maria and glassy mid-ocean ridge basalts, but, as far as we know, naturally occurring hollow alkali feldspar has not been reported previously. The morphology of both the hollow sanidine and hollow plagioclase is indicative of rapid growth from supersaturated melts. Unlike the lunar basalts and mid-ocean ridge basalts, loss of volatiles rather than heat probably induced supersaturation of the granitic melt. In contrast to the high Fe and Mg in hollow plagioclase, Fe and Mg in the hollow sanidine cannot be attributed to a $Ca(Fe,Mg)Si_3O_8$ component. To rationalize the sanidine analyses a $K_2(Fe,Mg)Si_7O_{16}$ feldspar component is proposed. If the proposed component is written in a more usual formulation based on 8 oxygens, it must be expressed as the sum of $[K(Mg,Fe^{2+})Si_3O_8]^-$ and $[KSi_4O_8]^+$. Charge balance of the component requires $(K,Na)^+$ occupancy of an octahedral site within a $[Si_4O_8]^0$ structural unit to compensate for the excess negative charge left unbalanced by $(K,Na)^+$ occupancy of an octahedral site within a $[(Fe,Mg)Si_3O_8]^{2-}$ unit.

The sanidine/granitic melt partition coefficient for Mg is estimated to be locally greater than five. The ratio of Mg in the sanidine to Mg in the mica peridotite is about 0.022. This value is close to previously reported feldspar/liquid Mg partition coefficients and implies that mica peridotite and granite melts achieved at least local metastable equilibrium.

Introduction

Mg-rich hollow sanidine, as much as 100 μm long, occur in blocks of Precambrian granite that are xenoliths in a Cretaceous mica peridotite exposed at Rose dome, Woodson County, Kansas (SE¼, sec. 13, T.26S., R.15E.) (Bickford et al., 1971; Franks et al., 1971). Insofar as we know, this is the first reported natural occurrence of hollow sanidine. Petrographic textures provide evidence that the granite was partially melted by the peridotite (Franks et al., 1971). The skeletal morphology of the sanidine microlites suggests growth from a melt that was supersatu-

rated with sanidine. Geological evidence indicates that supersaturation of the granitic partial melt primarily was induced by loss of volatiles from the peridotite-granite system, rather than by loss of heat. The hollow sanidine contains about 0.5 wt.% MgO. The content of MgO is much higher than that of other alkali feldspars, and suggests ion-exchange between the granitic melt and the peridotite. Moreover, the hollow sanidines not only contain about 1.5 wt.% FeO, but they also are unusually rich in Si and poor in Al, containing more than three Si cations per eight oxygens. The unique chemical composition implies local charge imbalance in the feldspar structure. The composition of the sanidine offers insight into the character of the interaction between the granitic partial melt and the host mica peridotite. The Mg-rich nature of the

---

[1] Present address: Amoco Production Company, Research Center, P.O. Box 3385, Tulsa, Oklahoma 74102.
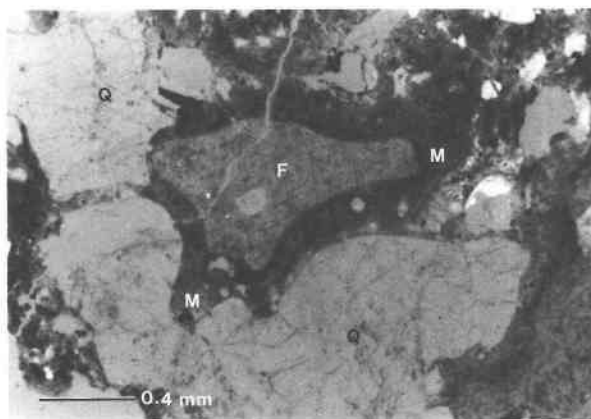
Fig. 1. Photomicrograph of Rose dome granite showing rounded relict grains of quartz (Q) and alkali feldspar (F) enclosed in microcrystalline matrix (M) of quartz and alkali feldspar crystallized from partial melt. Crossed polars.

Fig. 3. Photomicrograph of Rose dome granite showing hollow, equant, and lathlike sanidine (S) in felted matrix (M) composed chiefly of acicular feldspar but containing blebs of "limonite" (L) and scarce needlelike apatite (A). Plane-polarized light.

sanidine suggests that Mg-rich metasomatic fluids derived from the mica peridotite played an important role in their formation.

Textures

Melt textures

In parts of the granite, large subrounded to subangular grains of quartz and feldspar are separated by a fine-grained matrix (Fig. 1). The fine-grained matrix forms channels between the relict feldspar and quartz grains (Fig. 1) that appear similar to melt channels produced by experimental partial fusion of gneisses and granulites (Mehnert et al., 1973) and albite–quartz mixtures (Jurewicz and Watson,

1984). The observed distribution of relict grains and matrix is also similar to partially melted granulite xenoliths in the Lashaine kimberlite (Jones et al., 1983), and supports the conclusions of Franks et al. (1971) that the Rose dome granite was partially melted by the mica peridotite.

Crystallization textures

Much of the fine-grained matrix consists of micropoikilitic quartz that encloses tabular, lathlike, and skeletal sanidine microlites. Fretted sanidine laths occur on the margins of some remnant plagioclase (Fig. 2). Albite twinning is observed in some of the remnant grains, and the sanidine laths have nucleated and grown on alternate twins. Sanidine also forms rims on remnant K-feldspar grains, some of which show relict microcline twinning. Those sanidine crystals that did not nucleate on the margins of remnant feldspars form lathlike to equant and hollow
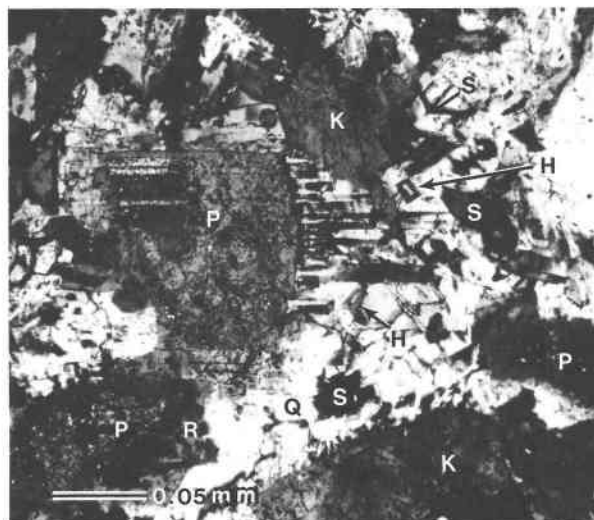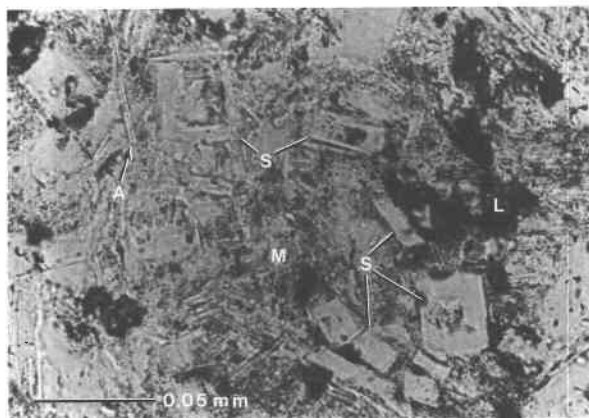

Fig. 2. Photomicrograph of Rose dome granite showing fretted, oriented overgrowths of sanidine (dark) near center of field. Fretted overgrowths are nucleated on and extended parallel to twin lamellae in relict plagioclase (P) at left of center. H, hollow sanidine; K, relict K-feldspar; R, overgrowth rim of sanidine on relict plagioclase (P) in lower left; Q, quartz; S, equant and lathlike sanidine. Crossed polars.
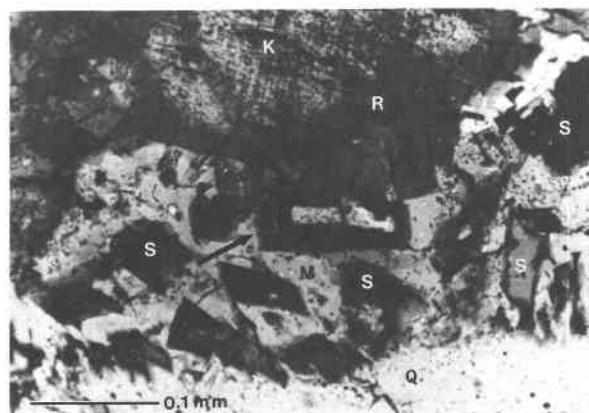

Fig. 4. Photomicrograph of Rose dome granite showing elongate, hollow sanidine (arrow) and equant to lathlike sanidine (S) poikilitically enclosed in matrix quartz (M) that is bordered by relict K-feldspar (K) and quartz (Q). Note sanidine rim (R) on relict K-feldspar. Crossed polars.

Table 1. K-feldspar compositions and optical properties. Points analyzed: A, B, hollow sanidine; C, D, E, F, hollow sanidine shown in Figures 4 and 5; G, hollow sanidine; H, relict K-feldspar

#	A	B	C	D	E	F	G	H
$2V_x$	$39\pm3°$			$40\pm2°$			$42\pm6°$	$<66°$
Microprobe analyses in weight per cent oxides								
SiO_2	66.4	67.5	66.1	67.5	66.2	66.0	66.6	65.0
Al_2O_3	15.2	15.2	14.7	15.4	15.2	14.8	15.7	18.4
CaO	0.07	0.03	0.01	0.00	0.18	0.04	0.01	0.06
FeO^*	1.53	1.36	1.35	1.52	1.33	1.55	1.01	0.04
MgO	0.49	0.46	0.44	0.52	0.45	0.53	0.52	0.00
K_2O	16.1	15.2	15.4	15.2	15.5	15.7	15.4	15.9
Na_2O	0.27	0.97	1.15	1.03	0.92	1.00	0.65	0.72
Total	100.1	100.7	99.2	101.2	99.7	99.6	99.9	100.1
* all iron reported as FeO								
Structural formulae in cations per 8 oxygens								
Si^{4+}	3.083	3.097	3.094	3.086	3.078	3.083	3.078	2.998
Al^{3+}	0.832	0.822	0.811	0.830	0.833	0.815	0.857	0.999
Fe^{2+}	0.059	0.052	0.053	0.058	0.052	0.061	0.039	0.001
Mg^{2+}	0.034	0.031	0.031	0.035	0.031	0.037	0.036	0.000
Ca^{2+}	0.003	0.001	0.001	0.000	0.009	0.002	0.000	0.003
Na^+	0.024	0.086	0.104	0.091	0.083	0.091	0.058	0.065
K^+	0.955	0.890	0.920	0.887	0.920	0.935	0.906	0.938
(IV)	4.008	4.002	3.989	4.009	3.994	3.996	4.010	3.998
(VI)	0.982	0.977	1.025	0.978	1.012	1.028	0.964	1.006
Total	4.990	4.979	5.014	4.987	5.006	5.024	4.974	5.004
(IV)=$Si^{4+}+Al^{3+}+Mg^{2+}+Fe^{2+}$; (VI)=$K^++Na^++Ca^{2+}$								

growths (Fig. 3). These sanidine microlites are clear and show no detectable sign of alteration. They mostly are enclosed in optically continuous micropoikilitic quartz, especially near the margins of relict quartz and feldspar (Fig. 4). Acicular and spherulitic sanidine and quartz intergrowths have been noted previously in the Rose dome granite (Franks et al., 1971), and other fine-grained samples of the granite, not considered in this study, contain altered mafic minerals. Na-rich feldspar has not been found in the fine-grained matrix.

To the best of our knowledge, naturally occurring hollow alkali feldspars have not been previously described. The morphology of the hollow sanidine is further evidence that Rose dome granite was partially melted, and that the fine-grained matrix is the recrystallized partial melt. The simple fact that hollow sanidines are found in the Rose dome granite, and that their morphology is indicative of growth from a supersaturated melt, is additional evidence that the granite was partially melted by the peridotite.

Optical studies

Measurements of $2V_x$ were made for six hollow and equant matrix feldspar grains using a Bausch and Lomb 5-axis universal stage. The measurements were corrected following the procedures of Emmons (1948). Corrected $2V_x$ values range from 37 to 54°, but only one of the measurements exceeds 44°. Orientation procedures and measurement of $2V_x$ were handicapped by the low birefringence and dark, first-order gray interference colors shown by the microlites cut nearly perpendicular to the acute bisectrix of the optic angle (Fig. 4). Consequently errors could be as large as $\pm3°$ for measurements of $1V_x$. $2V_x$ values for the grains analyzed using the microprobe are given in Table 1.

The hollow feldspar microlites have nearly euhedral shapes that range from equant to elongate when viewed down the acute bisectrix (Figs. 3 and 4). The orientation of the optic plane is about perpendicular to the long dimension of the elongate grains (Fig. 5). The optical data for the elongate hollow grains accord either with orthoclase crystals that are tabular parallel to {010} or with high sanidine that is elongate parallel to the **b** crystallographic axis or the trace of {001} (Smith, 1974; Su et al., 1984). X-ray diffraction and $2V$ studies of relict primary K-feldspar in Rose dome granite (Franks et al., 1971), however, are consistent with the thermal conversion of
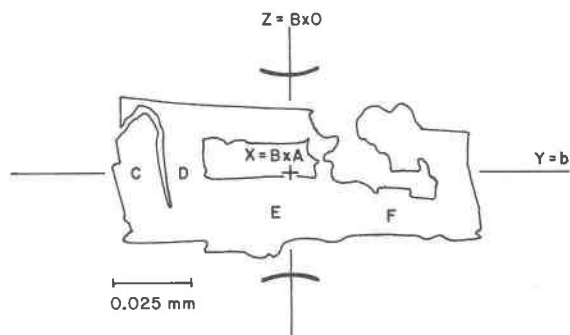
Fig. 5. Sketch of hollow sanidine (Fig. 4) showing approximate orientation of optical axes and inferred **b**-axis. Sketch not corrected for universal stage rotation. BxO, obtuse bisectrix. $2V = 40 \pm 4°$. C, D, E, and F mark locations of microprobe analyses in Table 1.

primary microcline to high sanidine after entrapment in the mica peridotite. The data from the relict feldspars combined with the textural evidence of partial melting (Fig. 1) and rapid crystallization (Figs. 3 and 4) support the inference that the hollow microlites are high sanidine, and that they commonly are elongate parallel to the trace of {001} in sections cut nearly perpendicular to the acute bisectrix or **a** crystallographic axis (Figs. 4 and 5). In contrast, the lathlike K-feldspar microlites (Figs. 2 and 3) are length fast, do not allow measurement of $2V_x$, and accord with elongation parallel to **a**.

Elongation parallel to **a** is characteristic of the rapidly crystallized plagioclase and alkali feldspar studied by Lofgren (1974, 1980), Bryan (1972), and Fenn (1977), whether or not the crystals are hollow. The shapes of hollow microlites in the Rose dome granite, then, differ significantly not only from the lathlike microlites in the granite, but also from the shapes of hollow feldspars studied by other workers. The hollow plagioclase studied by Bryan (1972) and most of the alkali feldspar grown by Fenn (1977) were tabular parallel to {010}. However, with increasing potassium content, the alkali feldspar grown by Fenn became less elongate parallel to **a**, less lathlike, and blocky due to ". . . a reduction in growth rate anisotropy along **c** and **a** . . . ." (Fenn, 1977, p. 152). Hence, although the hollow sanidine in the Rose dome granite differs significantly in morphology from previously reported hollow feldspars, their blocky, equant to elongate habit is analagous to Fenn's observations and consistent with their potassic compositions.

Feldspar compositions

Analytical procedures

Analyses were performed using an ARL-AMX electron microprobe operating at an acceleration potential of 15 kV and sample currents of 12–14 nA. the electron beam was focused to less than 3 μm in diameter. Standards were analyzed before and after each unknown. Counting times of ten seconds were employed. Five points were averaged for Si, Al, K, and Na, ten points for Ca, Mg, and Fe. The data were corrected for background; dead-time corrections were not required at the low sample currents used.

The data were reduced using the method of Bence and Albee (1969) and the correction factors of Albee and Ray (1970).

Microcline (K, Al, Si), anorthite (Ca), and osumilite (Fe, Mg) provided by the Smithsonian Institution (Jarosewich et al., 1980) and Amelia albite (Na) obtained from W. H. Taylor were used as standards. Na was also checked against the microcline standard. The osumilite used as the Fe and Mg standard has Si and Al contents very similar to K-feldspar and 4.00 wt.% K_2O. The only other major components of this standard are 6.38% FeO and 5.83% MgO. This standard was chosen for Fe and Mg to reduce possible errors associated with the correction procedures. Although much of the Rose dome granite is altered, the fine-grained sanidine-quartz matrix is very fresh. Many of the sanidine microlites are also sufficiently large to allow quantitative electron probe microanalyses (Fig. 4).

The analyzed hollow sanidines were fresh, showing no signs of alteration. The unaltered state of these feldspars, and the quality of the sanidine analyses can be judged using the sum of the oxide weight percents, which are all close to one hundred, and the structural formulae, all of which have close to five cations per eight oxygens, or a total of one octahedrally coordinated cation and four tetrahedrally coordinated cations per eight oxygens (Table 1). Further, the results of the analyses given in Table 1 are consistent between different hollow sanidines and within a single hollow sanidine. Also, our analysis of a relict potassium feldspar shows no compositional peculiarities (H, Table 1).

Feldspar compositions and tetrahedral substitutions

The compositions of three hollow sanidines and a relict K-feldspar are given in Table 1. The average structural formula for the seven analyses of the hollow feldspars is $(K_{0.916}Na_{0.077}Ca_{0.002})^{VI}(Mg_{0.034}Fe_{0.053}Al_{0.829}Si_{3.085})^{IV}O_8$. The structural formula indicates that the hollow sanidines are rich in Mg, Fe, and Si, and are depleted in Al relative to stoichiometric K-feldspar.

Because the sum of tetrahedrally coordinated cations per eight oxygens of all feldspars, whether stoichiometric or not, must be four, the data also suggest that Fe and Mg are tetrahedrally coordinated in the hollow sanidine (Table 1). Tetrahedral trivalent Fe is not uncommon in alkali feldspars, and feldspars of the composition $KFe^{3+}Si_3O_8$ have been synthesized (Faust, 1936; Wones and Appleman, 1963). Tetrahedrally coordinated divalent Fe and Mg occur in terrestrial and lunar plagioclase (Bryan, 1974; Longhi et al., 1973; Beatty and Albee, 1980; Crawford, 1972), and the partitioning of these two elements between plagioclase and liquid has been studied experimentally (Murphy, 1977; Longhi et al., 1976). These substitutions are attributed to feldspar components of the formula $CaMgSi_3O_8$ and $CaFe^{2+}Si_3O_8$. Plagioclase of both these compositions has been synthesized (Sclar and Kastelic, 1979; Sclar and Stead, 1980).

Although it may be argued that the iron in the hollow sanidine is trivalent, there is no ambiguity as to the valence state of magnesium. Therefore, the following discussion focuses mainly on the structural implications of Mg substitution in sanidine. Ferrous iron in sanidine, however, must occupy sites structurally similar to those occupied by Mg.

Ca is nearly absent in the sanidine. The atomic Mg/Ca ratio is greater than 10 (Table 1). Tetrahedral Mg and

Fe^{2+} in these feldspars cannot, therefore, be attributed to the magnesian and ferroan anorthite components discussed above. Rather, the chemical analyses and the calculated sanidine structural formulae can be rationalized by postulating a substitution of the feldspar component $(K,Na)_2(Mg,Fe^{2+})Si_7O_{16}$ into the hollow sanidine. This component requires that an octahedral site in a $[Si_4O_8]^0$ structural unit be occupied by an alkali cation (K^+) in order to satisfy the excess negative charge left unbalanced by the monovalent octahedral alkali cation in a $[(Mg,Fe^{2+})Si_3O_8]^{2-}$ structural unit.

Feldspars of the composition $(K,Na)_2(Mg,Fe)Si_7O_{16}$ have not been synthesized, but magnesian and ferroan analogues of leucite and kalsilite have (Roedder, 1951a,b, 1952). The synthesis of these compounds, moreover, documents the substitution of Mg^{2+} and Si^{4+}, or Fe^{2+} and Si^{4+}, for two tetrahedral Al^{3+} in potassic framework aluminosilicates.

High- and low-temperature polymorphs of $K_2MgSi_5O_{12}$ are isomorphous with high- and low-temperature leucite polymorphs, and the high- and low-temperature polymorphs of $K_2MgSi_3O_8$ are isomorphous with kalsilite and kaliophilite (Roedder, 1951a, 1951b). $K_2Fe^{2+}Si_5O_{12}$ and $K_2Fe^{2+}Si_3O_8$ are isomorphous with their magnesian counterparts (Roedder, 1952). Furthermore, there is complete solid solution between $K_2MgSi_5O_{12}$ and leucite (Schairer, 1948). The isomorphism and solid solution shown by these compounds accords with limited solid solution of $K_2(Mg,Fe^{2+})Si_7O_{16}$ in the disordered high-sanidine structure. The substitution of Mg^{2+} and Si^{4+} for two tetrahedral Al^{3+} cations may be thought of in terms of the reaction:

$$2\{KAlSi_3O_8\} + MgO + SiO_2$$
$$\rightleftharpoons Al_2O_3 + \{KMgSi_3O_8\}^- + \{KSi_4O_8\}^+.$$
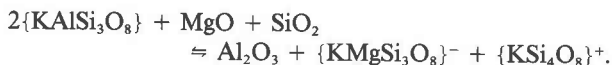
The average $K_2MgSi_7O_{16}$ content of these hollow sanidines is 6.8 wt.%. The mean $K_2FeSi_7O_{16}$ content is 11.2 wt.% if all iron is assumed to be ferrous. The Rose dome sanidines contain more than three silicon cations per eight oxygens (Table 1), and as far as we know are the most siliceous feldspars analyzed to date.

Discussion

Textures and morphology:
implications for petrogenesis

The best known occurrences of hollow feldspars are the calcic plagioclases in the glassy rims of mid-ocean ridge basalts (Bryan, 1972, 1974) and the lunar mare basalts (Crawford, 1972). These plagioclases, which tend to be sector zoned, grew from supercooled melts that result from the extrusion of anhydrous basalts into cold, deep-sea and lunar environments. Hollow plagioclase feldspars are not found in either subaerially erupted magmas or magmas erupted at shallow water depths (Bryan, 1974). Hollow plagioclases have been grown from the melt by Lofgren (1974, 1980) at linear cooling rates of 2°C per hour and in isothermal drop experiments resulting in supercoolings of 40 to 200°C.

Alkali feldspars grown from supercooled melts form

tabular crystals at small degrees of supercooling, and skeletal, dendritic, and spherulitic forms at progressively greater supercooling (Fenn, 1973, 1977; Swanson, 1977; Lofgren and Gooley, 1977). Fenn (1977) grew hollow alkali feldspars, having glass-filled cores, from supercooled hydrous alkali feldspar melts. Long (1978), in a study of the partitioning of Ba, Sr, and Rb between alkali feldspars and supercooled hydrous granitic melts, grew sector-zoned sanidine that appear to have small hollow cores (Long, 1978, Fig. 10).

The hollow feldspars in these previous studies crystallized from supersaturated melts. Although there are some morphological and chemical differences between the feldspars described in these previous studies and the hollow sanidine in the Rose dome granite, the gross similarities suggest that the latter also crystallized from a supersaturated melt.

Supersaturation of these other melts was thermally induced. Rapid cooling, however, probably does not account for hollow sanidine in Rose dome granite. The granite occurs as xenoliths in a mica peridotite that intruded the Pennsylvanian Stanton Limestone and Weston Shale, which probably were buried by 900 to 1200 m of younger rocks (Frank et al., 1971). Moreover, a considerable volume of hornfels was generated from the Weston Shale (Franks et al., 1971). It is probably a better approximation to infer nearly isothermal formation and crystallization of the molten matrix within the granite rather than a drop in temperature comparable to that experienced by mid-ocean ridge basalts and lunar basalts, even though loss of water from the melt may have been an efficient heat transport mechanism.

Supersaturation of hydrous feldspathic melts can be achieved with or without a drop in temperature through the loss of volatiles. The feldspar growth textures described here can be attributed to rapid loss of volatiles from the mica periodotite-granite system during emplacement at shallow crustal levels, perhaps at depths in the region of 900 to 1200 m (Franks et al., 1971). The presence of hornfels and metachert fragments in the outer parts of the partially melted granite xenoliths indicates that the matrix was molten during final emplacement of the mica peridotite. Moreover, the presence of hydrous and K-rich phases in buchite-like Weston hornfels and Stanton Limestone in contact with the peridotite indicates the transfer of water from the peridotite to the country rock during intrusion (Franks et al., 1971).

Mg in sanidine: comparison with other feldspars

The MgO content of the sanidine microlites, 0.44 to 0.53 wt.%, is similar to that of hollow sector zoned plagioclase in the glassy rims of submarine pillow basalts, 0.24–0.54 wt.%, reported by Bryan (1974) but it is unusually high compared to other alkali feldspars. For example, 31 alkali feldspars analyzed by De Pieri et al. (1977) all have MgO less than 0.04 wt.%. Eight sanidines analyzed by Basu and Vitaliano (1976) all have less than 0.03 wt.% MgO. Eighteen anorthoclase megacrysts analyzed by

Mason et al. (1982) using an ion microprobe all have between 2 and 52 parts per million Mg by weight. The albite and K-feldspar phases of seven perthites from four pegmatites analyzed using an ion microprobe all have less than 11 parts per million Mg by weight (Mason, 1982). Data on Mg is also absent in the recent paper of Schearer et al. (1985) on the major and trace element compositions of potassium feldspars from three pegmatites in the Black Hills.

The normally insignificant amount of MgO in sanidine, and other alkali feldspars as well, also is reflected in the absence of data on Mg in the sanidine/glass partition coefficients published by Leeman and Phelps (1981) and Mahood and Hildreth (1983). The unusual amounts of Mg in the matrix sanidine, however, doubtless reflect partitioning of Mg between the interstitial granitic melt in the xenoliths and the mica peridotite.

Mg-partitioning between feldspars and melts

Estimation of the partition coefficients between the Rose dome matrix sanidine and the mica peridotite offers insight into the nature of the interaction between the granitic partial melt and the mica peridotite, as well as into the possible importance of Mg-rich metasomatic fluids derived from the mica peridotite melt. Although the distribution of quartz and feldspar is highly variable in the recrystallized partial granitic melts, we estimate a quartz to sanidine ratio of about four to one where the sanidine is enclosed in quartz. Minor apatite is the only other phase in the fine-grained matrix we studied. Sanidine is the only matrix phase that contains appreciable Mg in our samples. The sanidine/whole-matrix Mg partition coefficient is, therefore, estimated to be about 5. The sanidine/granite-melt Mg partition coefficient must be greater than 5, especially because the melt probably was water saturated (Franks et al., 1971).

In contrast, a number of studies indicate that feldspar/melt Mg partition coefficients generally are less than one. The Mg mineral/matrix partition coefficient of 12 homogenous alkali feldspars determined by De Pieri and Quareni (1978) range from 0.00 to 0.33. These values are based on chemical analyses of feldspar and glass separates and the higher values may be in excess of the actual partition coefficients because of impurities and inclusions in the feldspars. Ion microprobe analyses of an anorthoclase megacryst from Mt. Erebus, Antarctica, and a glass inclusion within the megacryst yield an anorthoclase/glass Mg partition coefficient of 0.008 (Mason et al., 1982). Using electron microprobe data Longhi et al. (1976) demonstrated that the Mg plagioclase/liquid partition coefficients for low-Ti lunar basalts and terrestrial basalts are about 0.041.

The large feldspar/melt Mg partition coefficient estimated for the hollow sanidine could reflect rapid growth from the melt, consistent with the hollow character of the microlites. Schiffman and Lofgren (1981), for example, documented an increase in iron concentration in andesine from the range 0.66–0.69 to the range 1.56–2.55 wt.% as the cooling rates of a basaltic melt were changed from 0.5°C per hour to 218°C per hour. They attributed this increase of Fe content to kinetic effects of Fe entrapment at the plagioclase–liquid interface. However, even though the Fe plagioclase/liquid partition coefficient increased sympathetically with cooling rate in these experiments, it never exceeded unity, and rapid growth does not appear to be the sole factor responsible for the high Mg content of the Rose dome sanidine.

Mineral/liquid partition coefficients are also a function of both crystal structure (Philpotts, 1978; Takahashi and Irvine, 1981) and melt structure (Watson, 1976, 1977; Hart and Davis, 1978; Ryerson and Hess, 1978; Mahood and Hildreth, 1983). Relative values of partition coefficients of two isovalent elements that occupy the same crystallographic site primarily are controlled by the crystal structure (Philpotts, 1978). The absolute value of a mineral/liquid partition coefficient, however, is primarily a function of liquid structure. In general, the mineral/melt partition coefficient of a network-modifying cation, such as Mg, increases sympathetically with melt polymerization. This effect is clearly illustrated in the partitioning of network-modifying cations among minerals in equilibrium with a strongly depolymerized Fe-rich melt and a highly polymerized Si-rich melt. The mineral/melt partition coefficients are much larger for the Si-rich melt than for the equilibrium Fe-rich melt (Watson, 1976; Ryerson and Hess, 1978). The nonequlibrium partitioning of elements between the silica-undersaturated ultramafic mica peridotite and the granitic melt may approximate the equilibrium distribution of elements between low-temperature Fe- and Si-rich immiscible liquids.

Although the sanidine/granite-melt Mg partition coefficient is greater than one, the sanidine/mica peridotite Mg partition coefficient must be much less than one. The MgO content of one sample of noncalcareous Rose dome mica peridotite is 22.31 weight percent (Franks et al., 1971). Using this value as an order of magnitude estimate of the Mg content of the mafic alkaline melt yields a sanidine/mica-peridotite Mg partition coefficient of 0.022. This value is about three times that of the anorthoclase/glass partition coefficient (0.008) determined by Mason et al. (1982), about one half of the plagioclase/basaltic–liquid Mg partition coefficient (0.041) of Longhi et al. (1976), and within the range of the alkali-feldspar/matrix Mg partition coefficients (0.00–0.33) of De Pieri and Quareni (1978). The similarity of the hollow-sanidine/mica-peridotite Mg partition coefficient to other feldspar/melt pairs suggests that the distribution of elements between the granite partial melt and the mica-peridotite melt enclosing the granite xenoliths achieved metastable equilibrium, even though no peridotite melt permeated deeply into the xenoliths studied by us.

The similarity of the MgO content of Rose dome hollow sanidine to the hollow plagioclase grown from relatively MgO-rich mid-ocean ridge basalts may be due to the interaction between the granite and Mg-rich metasomatic fluids derived from the peridotite. Isolated phlogopite

crystals that grew within limestone xenoliths in the peridotite (Franks et al., 1971) support the idea of K- and Mg-rich metasomatic fluids. A metosomatic fluid phase would have greatly facilitated ion-exchange between the granitic melt and the peridotite and favored crystallization of Mg-rich sanidine.

Mg in sanidine: crystal chemical implications

The Mg-, Si-rich sanidine compositions presented here are the first unambiguous evidence of local charge imbalance within individual four member tetrahedral ring units in feldspar. Our documentation of the $[KSi_4O_8]^+$ and $[KMgSi_3O_8]^-$ feldspar components opens the door for speculation on local charge imbalance in feldspars of more usual composition. Possible charged components in alkali feldspar are $[(Na,K)Si_4O_8]^+$ and $[(Na,K)Al_2Si_2O_8]^-$. The components $[CaAlSi_3O_8]^+$ and $[NaAl_2Si_2O_8]^-$ may occur in plagioclase. In all cases, equal numbers of positively and negatively charged units are required in the crystal structure if overall charge balance is to be maintained. Betterman and Liebau (1976) synthesized feldspars of the formula $LaNaAl_4Si_4O_{16}$. The application of the Al-avoidance principle, which states that $[AlO_4]^{5-}$ tetrahedra do not share corners (Smith, 1974) to this feldspar implies the existence of $[LaAl_2Si_2O_8]^+$ and $[NaAl_2Si_2O_8]^-$ components. The possibility of local charge imbalance between 4-member ring units in feldspars, and, hence, additional substitutional disorder probably ought to be included in atomistic models of the feldspar structures.

Conclusions

1. Mg-rich hollow sanidine in the Rose dome granite probably grew from a supersaturated melt.

2. Supersaturation of the granitic partial melt probably was induced by loss of volatiles rather than loss of heat.

3. The sanidine/granitic melt Mg partition coefficient is greater than five, indicating ion-exchange between the granitic melt and the mica peridotite that enclosed the granite xenoliths.

4. Ion exchange between the granitic melt and mica peridotite probably was facilitated by K- and Mg-rich metasomatic fluids.

5. The sanidine compositions indicate the exisitence of a $K_2MgSi_7O_{16}$ feldspar component, and document the occurrence of local charge imbalance in feldspar.

Acknowledgments

References

Albee, A. L. and Ray, L. (1968) Correction factors for electron probe microanalysis of silicates, oxides, carbonates, and sulfates. Analytical Chemistry, 42, 1408–1414.

Basu, A. and Vitaliano, C. J. (1976) Sanidine from the Mesa Falls Tuff, Ashton, Idaho. American Mineralogist, 61, 405–408.

Bence, A. E. and Albee, A. L. (1968) Empirical correction factors for the electron microanalysis of silicates and oxides. Journal of Geology, 76, 382–403.

Betterman, P. and Liebau, F. (1976) Lanthanum–calcium–sodium aluminosilicates $La_xCa_{8-2x}Na_x[Al_{16}Si_{16}O_{64}]$. Naturwissenschaften, 63, 480.

Bickford, M. E., Mose, D. G., Wetherhill, G. W., and Franks, P. C. (1971) Metamorphism of Precambrian granitic xenoliths in a mica peridotite at Rose Dome, Woodson County, Kansas: Part 1, Rb–Sr isotopic studies. Geological Society of America Bulletin, 82, 2863–2868.

Bryan, W. B. (1972) Morphology of quench crystals in submarine basalts. Journal of Geophysical Research, 77, 5812–5819.

Bryan, W. B. (1974) Fe–Mg relationships in sector-zoned submarine basalt plagioclase. Earth and Planetary Science Letters, 24, 157–165.

Crawford, M. L. (1973) Crystallization of plagioclase in mare basalts. Proceedings of the Fourth Lunar Science Conference, 705–717.

De Pieri, R., De Vecchi, G., Gregnanin, A., and Piccirillo, E. M. (1977) Trachyte and rhyolite feldspars in the Euganean hills (northern Italy). Memorie degli Instituti di Geologia e Mineralogia dell'Universita di Padova.

De Pieri, R. and Quareni, S. (1978) Partition coefficients of alkali and alkaline-earth elements between alkali feldspar phenocrysts and their lava matrix. Mineralogical Magazine, 42, 63–67.

Emmons, R. C. (1943) The univeral stage. Geological Society of America Memoir 8.

Faust, G. T. (1936) The fusion relations of iron-orthoclase, with a discussion of the evidence of the existence of an iron-orthoclase molecule in feldspars. American Mineralogist, 21, 735–763.

Fenn, P. M. (1973) Nucleation and growth of alkali feldspars from melts in the system $NaAlSi_3O_8$–$KAlSi_3O_8$–H_2O. Ph.D. Thesis, Stanford University, Palo Alto.

Fenn, P. M. (1977) The nucleation and growth of alkali feldspars from hydrous melts. Canadian Mineralogist, 15, 135–161.

Franks, P. C., Bickford, M. E., and Wagner, H. C. (1971) Metamorphism of Precambrian granitic xenoliths in a mica peridotite at Rose Dome, Woodson County, Kansas: part 2, petrologic and mineralogic studies. Geological Society of America Bulletin, 82, 2869–2890.

Hart, S. R. and Davis, K. E. (1978) Nickel partitioning between olivine and silicate melt. Earth and Planetary Science Letters, 40, 203–219.

Jarosewich, E., Nelen, J. A., and Norberg, J. A. (1980) Reference samples for electron microprobe analysis. Geostandards Newsletter, 4, 43–47, 257.

Jones, A. P., Smith, J. V., Dawson, J. B., and Hansen, E. C. (1983) Metamorphism, partial melting, and K-metasomatism of garnet-scapolite-kyanite granulite xenoliths from Lashaine, Tanzania. Journal of Geology, 91, 143–165.

Jurewicz, S. R. and Watson, E. B. (1984) Distribution of partial melt in a felsic system: the importance of surface energy. Contributions to Mineralogy and Petrology, 85, 25–29.

Leeman, W. P. and Phelps, D. W. (1981) Partitioning of rare earths and other trace elements between sanidine and coexisting volcanic glass. Journal of Geophysical Research, 86, 10193–10199.

Lofgren, G. (1974) An experimental study of plagioclase crystal morphology: isothermal crystallization. American Journal of Science, 274, 243–273.

Lofgren, G. (1980) Experimental studies on the dynamic crystallization of silicate melts. In R. B. Hargraves, Ed., Physics

of Magmatic Processes, p. 487–551. Princeton University Press, Princeton.

Lofgren, G. E. and Gooley, R. (1977) Simultaneous crystallization of feldspar intergrowths from the melt. American Mineralogist, 62, 217-228.

Long, P. E. (1978) Experimental determination of partition coefficients for Rb, Sr, and Ba between alkali feldspar and silicate liquid. Geochimica et Cosmochimica Acta, 42, 833–846.

Longhi, J., Walker, D., and Hays, J. F. (1976) Fe and Mg in plagioclase. Proceedings of the Seventh Lunar Science Conference, 1281–1300.

Mahood, G. and Hildreth, W. (1983) Large partition coefficients for trace elements in high-silica rhyolites. Geochimica et Cosmochimica Acta, 47, 11–30.

Mason, R. A. (1982) Trace element distributions between the perthite phases of alkali feldspars from pegmatites. Mineralogical Magazine, 45, 101–106.

Mason, R. A., Smith, J. V., Dawson, J. B., and Treves, S. B. (1982) A reconnaissance of trace elements in anorthoclase megacrysts. Mineralogical Magazine, 46, 7–11.

Mehnert, K. R., Busch, W., and Schneider, G. (1973) Initial melting at grain boundaries of quartz and feldspar in gneisses and granulites. Neues Jarbuch für Mineralogie Monatshefte, 165–183.

Murphy, W. M. (1977) An experimental study of solid-liquid equilibria in the albite-anorthite-diopside system. M.S. Thesis, University of Oregon, Eugene.

Philpotts, J. A. (1978) The law of constant rejection. Geochimica et Cosmochimica Acta, 42, 909–920.

Roedder, E. W. (1951a) The system $K_2O–MgO–SiO_2$ part 1. American Journal of Science, 249, 81–130.

Roedder, E. W. (1951b) The system $K_2O–MgO–SiO_2$ part 2. American Journal of Science, 249, 224–248.

Roedder, E. W. (1952) A reconnaissance of liquidus relations in the system $K_2O \cdot 2SiO_2–FeO–SiO_2$. American Journal of Science, Bowen Volume, 435–456.

Ryerson, F. J. and Hess, P. C. (1978) Implications of liquid–liquid distribution coefficients to mineral–liquid partitioning. Geochimica et Cosmochimica Acta, 42, 921–932.

Schairer, J. F. (1948) Phase equilibrium relations in the quaternary system $K_2O–MgO–Al_2O_3–SiO_2$ (preliminary report). Geological Society of America Meeting, New York, November 1948 (not seen; extracted from Roedder, 1951b).

Schiffman, P. and Lofgren, G. E. (1982) Dynamic crystallization studies on the Grande Ronde pillow basalts, central Washington. Journal of Geology, 90, 49–78.

Sclar, C. B. and Kastelic, R. L. (1979) Iron in anorthite: synthesis and characterization of the $CaAl_2Si_2O_8–CaFeSi_3O_8$ series. (abstr.) Transactions of the American Geophysical Union (EOS), 60, 421.

Sclar, C. B. and Stead, R. J. (1981) Kinetics of synthesis and disproportionation reactions of $CaMgSi_3O_8$. (abstr.) Transactions of the American Geophysical Union (EOS), 62, 410.

Sheerer, C. K. and Papike, J. J. (1985) Chemistry of potassium feldspars from three zoned pegmatites, Black Hills, South Dakota: implications concerning pegmatite evolution. Geochimica et Cosmochimica Acta, 49, 663–673.

Smith, J. V. (1974) Feldspar Minerals, Volume 1. Springer-Verlag, New York.

Snyder, J. L. (1962) Geologic investigations, Central Davis Mountains, Texas. Texas Journal of Science, 14, 197–215.

Su, S. C., Bloss, F. D., Ribbe, P. H., and Stewart, D. B. (1984) Optic axial angle, a precise measure of Al,Si ordering in the T_1 tetrahedral sites of K-rich alkali feldspars. American Mineralogist, 69, 440–448.

Swanson, S. E. (1977) Relation of nucleation and crystal-growth rate to the development of granitic textures. American Mineralogist, 62, 966–978.

Takahashi, E. and Irvine, T. N. (1981) Stoichiometric control of crystal/liquid single-component partition coefficients. Geochimica et Cosmochimica Acta, 45, 1181–1185.

Watson, E. B. (1976) Two liquid partition coefficients: experimental data and geochemical implications. Contributions to Mineralogy and Petrology, 56, 119–134.

Watson, E. B. (1977) Partitioning of manganese between forsterite and silicate liquid. Geochimica et Cosmochimica Acta, 41, 1363–1374.

Wones, D. R. and Appleman, D. E. (1963) Properties of synthetic triclinic $KFeSi_3O_8$, iron-microcline, with some observations on the iron-microcline=iron-sanidine transition. Journal of Petrology, 4, 131–137.